

# The two-gap BCS model in the large- $N$ approximation within a field-theory approach.

Leandro O. Nascimento<sup>1\*</sup>

<sup>1</sup> *Faculdade de Ciências Naturais, Universidade Federal do Pará, C.P. 68800-000, Breves, PA, Brazil.*

(Dated: May 4, 2021)

We study the continuum version of the two-gap BCS model in (3+1)D within the large- $N$  approximation. We calculate the effective potential of the model which depends on two independent energy gaps  $\sigma$  and  $\Delta$ , where  $\sigma$  describes the Cooper pair made of electrons that belong to the same flavor whereas  $\Delta$  describes the Cooper pair of electrons that belong to different flavors. The effective potential is calculated by considering that the Debye frequency is an ultraviolet cutoff  $\Lambda$ , which is meant to describe the physical lattice of 3D superconductors. Our main result establishes a critical gap  $\Delta_0^c$  above which the system is in the normal phase where  $\sigma_0 = \langle \sigma \rangle = 0$  and below the system is in the superconductor phase. Furthermore, we also show that  $\Delta_0^c$  defines the energy scale for the critical temperature  $T_{c2} \approx \Delta_0^c e^{\gamma_E} / \pi$  of  $\sigma_0$ , where  $\gamma_E \approx 0.57$  is the Euler constant. Our results are likely to be relevant for describing two-gap superconductors, such as MgB<sub>2</sub> and underdoped cuprates, within a field-theory perspective. Furthermore, it may be relevant for studying steady-state superconductivity in lower dimension.

Subject Areas: Quantum Field Theory, Quantum critical phenomena (superconductivity), BCS theory (superconductivity).

PACS numbers: 03.70.+k, 74.40.Kb, 74.20.Fg,

## I. INTRODUCTION

The theoretical description of quantum states of matter usually relies on the investigation of spontaneous symmetry breaking either in quantum field theory (QFT) [1–3] or condensed matter physics (CMP) [4, 5]. In both cases, it is the so-called effective potential that provides a gap equation, i.e., the equation for the order parameter. The BCS-superconductivity of 3D-semiconductors is one famous example of such description [6] within CMP. Obviously, due to the presence of the crystal lattice as well as the inherent many-body problem, one may apply first-principle methods, such as the density functional theory [7]. Conversely, one also may consider a microscopic description in terms of quasiparticles, which allow us to obtain a precise and simplified view of the problem [4, 5]. This description allow us to include electronic interactions within a QFT perspective, as it has been done in Refs. [8, 9], where an effective model is built for describing quantum states of matter in two-dimensional materials [10–12]. Within this approach, the crystal lattice is only defined by the lattice parameter  $a$ , which defines the ultraviolet cutoff  $\Lambda \propto 1/a$ . Interesting, it is well known that the BCS model also admits such simplified description as it has been recently reviewed in Ref. [5].

The physical properties of a superconductor, within the BCS theory [6], are explained by a spontaneous Gauge-symmetry breaking due to the formation of Cooper pairs, i.e., the pairing of electrons with opposite momentum and spins. This occurs when mechanical vibrations become stronger than electronic repulsion at low temperatures, below a certain critical value  $T_c$ . Within this phase, magnetic fields are expelled by the material, which is known as Meissner-Ochsenfeld effect, and the application of a strong magnetic field lead the material

to the normal phase. On the other hand, the theoretical explanation of high-temperature superconductivity remains a open question [4, 5, 13, 14]. In this context, new models and experiments have been proposed, in particular, for describing the contribution of an anisotropy in the electron-electron pairing, which is sometimes called a two-gap superconductor [15–17].

The two-gap BCS model has been applied for describing underdoped cuprate superconductors in Ref. [15] with a momentum-dependent interaction. The main idea is to find a larger critical temperature due to the formation of two energy gaps, where the first one describes the pairing of electrons with small Fermi velocity while the second gap describes the pairing of electrons with large Fermi velocity. These electrons are expected to occur at some high-symmetry points of the Brillouin zone [15]. An extra example of unconventional pairing of electrons has been shown to occur in the honeycomb lattice. In this case, a nonequilibrium superconductivity emerges due to the pairing of electrons that belong to different *valleys* and *bands*. This phase may be achieved by the application of circular-polarized light into the material, which is able to select electrons in a specific valley. Furthermore, it is expected a critical temperature larger than its equilibrium value [18].

Here, we propose a field-theory approach to describe a flavor symmetry breaking in the BCS model, which implies a two-gap phase. Our approach, nevertheless, neglects the underlying mechanism for the flavor symmetry breaking, which is assumed to be generated by an external field, similar to the polarized light in the case of states out of equilibrium [18]. Thereafter, we use the Hubbard-Stratonovich transformation for obtaining a trilinear action with two auxiliary fields  $\sigma$  and  $\Delta$ . Integrating out the fermions and considering a constant-field

configuration, we derive the so-called effective potential of the model, which is dependent on these two fields. From this potential, we derive a set of two coupled-gap equations, which allows to calculate the vacuum expectation values of  $\sigma$  and  $\Delta$ . From the gap equations, we obtain a critical gap  $\Delta_0^c$  which separates the normal phase from the superconductor phase. Furthermore, we calculate the critical temperature for  $\sigma_0 = \langle \sigma \rangle$  in terms of  $\Delta_0^c$ .

The outline of this paper is the following: in Sec. II we apply our field-theory approach to the standard BCS model in order to review our main steps. In Sec. III we apply the large- $N$  approximation to the two-gap BCS model. In Sec. IV we discuss our main results. We also include an appendix where we give some details regarding the effective action in the large- $N$  approximation.

## II. THE CONTINUUM LIMIT OF THE BCS THEORY

In this section we apply the large- $N$  expansion [2] for the *continuum* limit of the BCS model in order to derive the gap equation as well as the critical temperature. In order to do so, let us start with the action [5], given by

$$\mathcal{L}_{\text{BCS}} = \psi_{sa}^* \left( i \frac{\partial}{\partial t} + \frac{\nabla^2}{2m} \right) \psi_{sa} - \frac{\lambda}{N} \psi_{\uparrow a}^* \psi_{\downarrow a}^* \psi_{\downarrow a} \psi_{\uparrow a}, \quad (1)$$

where  $s = \uparrow, \downarrow$  describes the spin and  $a = 1, \dots, N$  is a flavor index. The matter field  $\psi_{sa}$  describes the electronic excitation in a 3D-semiconductor with parabolic energy dispersion, namely,  $\xi_k = \mathbf{k}^2/2m$ , where  $m$  is the effective mass of the quasiparticle. The coupling constant  $\lambda$  is meant to describe the electron-phonon interaction. We assume that there exist  $N$  fields, such that we are allowed to use the large- $N$  expansion in Eq. (1). For the sake of simplicity, we shall consider  $\hbar = 1$ .

It is well known that we can convert the quartic interaction in Eq. (1) into a trilinear one, using the Hubbard-Stratonovitch transformation with an auxiliary field  $\sigma(x)$  [2]. Hence,

$$\mathcal{L}_{\text{BCS}} \rightarrow \mathcal{L}_{\text{BCS}} + \frac{N}{\lambda} \left( \sigma + \frac{\lambda}{N} \psi_{\uparrow a}^* \psi_{\downarrow a}^* \right) \left( \sigma^* + \frac{\lambda}{N} \psi_{\downarrow a} \psi_{\uparrow a} \right). \quad (2)$$

On the other hand, the motion equation for  $\sigma$  is given by

$$\frac{\delta \mathcal{L}_{\text{BCS}}}{\delta \sigma^*} \Big|_{\sigma = \sigma_0} = 0. \quad (3)$$

Using Eq. (2) in Eq. (3), we find

$$\sigma_0 = -\frac{\lambda}{N} \langle \psi_{\uparrow a}^* \psi_{\downarrow a}^* \rangle, \quad (4)$$

which is our order parameter for the phase transition. Indeed, despite the fact that the action in Eq. (1) is invariant under the gauge transform  $\psi_{sa} \rightarrow e^{i\alpha} \psi_{sa}$ , the

vacuum state breaks this symmetry when  $\sigma_0 \neq 0$ , accordingly to Eq. (4). In particular, for  $\sigma_0 \neq 0$ , the system exhibits a pair of bounded electrons with opposite spins, the so-called Cooper pairs [4].

From Eq. (2), we have our large- $N$  version of the continuum BCS theory, namely,

$$\begin{aligned} \mathcal{L}_{\text{BCS}} &= \psi_{sa}^* \left( i \frac{\partial}{\partial t} + \frac{\nabla^2}{2m} \right) \psi_{sa} \\ &+ \frac{N|\sigma|^2}{\lambda} + \sigma \psi_{\downarrow a} \psi_{\uparrow a} + \sigma^* \psi_{\uparrow a}^* \psi_{\downarrow a}^*. \end{aligned} \quad (5)$$

Eq. (5) is useful for calculating both the effective potential and the effective action (See App. A for more details) in the large- $N$  limit, as we shall discuss.

### II.A-The Effective Potential

Firstly, we note that Eq. (5) may be written as a quadratic action, hence,

$$\begin{aligned} \mathcal{L}_{\text{BCS}} &= \Phi_a^\dagger \begin{pmatrix} i \frac{\partial}{\partial t} + \frac{\nabla^2}{2m} & \sigma \\ \sigma^* & i \frac{\partial}{\partial t} - \frac{\nabla^2}{2m} \end{pmatrix} \Phi_a \\ &+ \frac{N|\sigma|^2}{\lambda}, \end{aligned} \quad (6)$$

where the Nambu fermion field is given by a two-component field, namely,  $\Phi_a^\dagger = (\psi_{\uparrow a}^* \psi_{\downarrow a})$ . Fortunately, Eq. (6) is quadratic in  $\Phi_a$ .

$$\mathcal{L}_{\text{BCS}} = \Phi_a^\dagger \hat{K} \Phi_a + \frac{N|\sigma|^2}{\lambda}, \quad (7)$$

where

$$\hat{K} = \begin{pmatrix} i \frac{\partial}{\partial t} + \frac{\nabla^2}{2m} & \sigma \\ \sigma^* & i \frac{\partial}{\partial t} - \frac{\nabla^2}{2m} \end{pmatrix}. \quad (8)$$

The partition function of the model reads

$$Z = \int D\Phi_a^\dagger D\Phi_a D\sigma e^{iS_{\text{BCS}}[\Phi_a, \sigma]}. \quad (9)$$

The integration over  $\Phi_a$  is solved with the help of the following property [4]

$$\int D\Phi_a^\dagger D\Phi_a e^{-\int d^4x \Phi_a^\dagger \hat{G} \Phi_a} = \exp\{N \ln \det \hat{G}\}, \quad (10)$$

where  $\hat{G}$  is an arbitrary matrix. Therefore Eq. (10), yields

$$Z = \int D\sigma e^{i \int d^4x \mathcal{L}_{\text{eff}}[\sigma]}, \quad (11)$$

where the effective action for  $\sigma$  reads

$$\mathcal{L}_{\text{eff}}[\sigma] = \frac{N|\sigma|^2}{\lambda} - iN \ln \det \{-i\hat{K}[\sigma]\}. \quad (12)$$

On the other hand, the effective potential  $V_{\text{eff}}[\sigma]$  is obtained through  $\mathcal{L}_{\text{eff}}[\sigma]$  when we consider a constant-field configuration, i.e,  $\sigma(x) = \sigma$ , where  $\sigma$  is not dependent on space-time coordinates [4]. Having this in mind, it follows that

$$Z = \int D\sigma e^{i \int d^4x \mathcal{L}_{\text{eff}}[\sigma]} \rightarrow \int D\sigma e^{i V_{\text{eff}}[\sigma] \Omega}, \quad (13)$$

where  $\Omega$  is an arbitrary space-time volume of quantization. From Eq. (8), it is straightforward to show that  $\det \{-i\hat{K}[\sigma]\} = -\omega^2 + \xi_k^2 + |\sigma|^2$ . Hence, using Eq. (12) in Eq. (13), we find

$$V_{\text{eff}}[\sigma] = \frac{N|\sigma|^2}{\lambda} - iN \int \frac{d^4k}{(2\pi)^4} \ln(-\omega^2 + \xi_k^2 + |\sigma|^2), \quad (14)$$

where  $d^4k = d\omega d^3\mathbf{k}$  and  $\xi_k = \mathbf{k}^2/2m$ . Note that the last term in the rhs of Eq. (14) is the Fourier transform of  $\ln \det \{-i\hat{K}[\sigma]\}$  for  $\sigma(x) = \sigma$ . From Eq. (14), it is clear that the effective potential is invariant under the transform  $\sigma \rightarrow -\sigma$ , therefore, the vacuum state is expected to be double degenerated. This is the same feature shown by a generic Landau-Ginzburg potential [4], as we shall prove later.

## II.B-The Gap Equation

The gap equation is obtained by extremizing the effective potential, i.e.,

$$\frac{\partial V_{\text{eff}}}{\partial \sigma} \Big|_{\sigma=\sigma_0} = V'[\sigma_0] = 0. \quad (15)$$

Using Eq. (14), we find

$$-\frac{1}{\lambda} = i \int \frac{d^4k}{(2\pi)^4} \frac{1}{\omega^2 - \xi_k^2 - |\sigma_0|^2}. \quad (16)$$

After integrating over  $\omega$  in Eq. (16), we obtain

$$-\frac{1}{\lambda} = -\frac{1}{2} \int \frac{d^3k}{(2\pi)^3} \frac{1}{\sqrt{\xi_k^2 + |\sigma_0|^2}}, \quad (17)$$

which is the so-called BCS gap equation [4]. Obviously, Eq. (17) is divergent for  $k \rightarrow \infty$ , as it usually is the case for gap equations. We shall circumvent this problem by considering an ultraviolet cutoff  $\Lambda$ .

Note that the integral variable may be written as

$$\frac{d^3k}{(2\pi)^3} = N_s D(\xi_k) d\xi_k, \quad (18)$$

where

$$D(\xi_k) = \frac{(2m)^{3/2} \xi_k^{1/2}}{4\pi^2} \quad (19)$$

is the density of states,  $\xi_k = \mathbf{k}^2/2m$ , and  $N_s = 2$  is the spin degeneracy. The standard approximation for the BCS model is to consider that  $D(\xi_k) \approx D(k_F) = mk_F/2\pi^2$ , where  $k_F$  is the Fermi momentum.  $D(k_F)$  is, therefore, the density of states at the Fermi surface of the metallic state. It turns out that for a metal  $k_F \approx 10^4 \text{K}$  in units of temperature. On the other hand, phonons may only transfer energy close to the Debye frequency  $\omega_D \propto 1/a \approx 10^2 \text{K}$ , where  $a$  is the lattice parameter. Therefore, we conclude that the integral may be calculated in the interval  $\xi_k \in [0, \omega_D] \equiv [0, \Lambda]$ , where  $\Lambda = \omega_D$  is an ultraviolet cutoff. We conclude, based on these numbers, that most of the electrons are not affected by this interaction, except those who are close to the Fermi energy. This explains our approximation into integral over  $k$ , hence, it follows that [4, 5]

$$\int \frac{d^3k}{(2\pi)^3} \rightarrow \int_0^{\omega_D} d\xi_k N_s D(k_F). \quad (20)$$

Using Eq. (20) in Eq. (17), we find

$$\frac{1}{\lambda} \approx \int_0^{\Lambda} d\xi_k \frac{D(k_F)}{\sqrt{\xi_k^2 + |\sigma_0|^2}} = D(k_F) \sinh^{-1} \left[ \frac{\Lambda}{|\sigma_0|} \right]. \quad (21)$$

Finally, because  $\sinh^{-1}[\Lambda/|\sigma_0|] \approx \ln[2\Lambda/|\sigma_0|]$  for  $\Lambda \gg |\sigma_0|$ , we find

$$|\sigma_0| \approx 2\Lambda e^{-1/\lambda D(k_F)}, \quad (22)$$

which is the BCS gap for a superconductor.

Note that, by comparison between Eq. (16) and Eq. (21), we may summarize all of our approximations by using

$$i \int \frac{d^4k}{(2\pi)^4} \frac{1}{\omega^2 - \xi_k^2 - |Z|^2} \approx -D(k_F) \ln \left( \frac{2\Lambda}{|Z|} \right) \quad (23)$$

for any  $Z$  and  $\Lambda \gg |Z|$ . Eq. (23) is very useful for our purposes. Indeed, it allow us to easily find an analytical expression for  $V_{\text{eff}}[\sigma]$  in Eq. (14).

We assume that  $\sigma$  is real, such that  $|\sigma|^2 = \sigma^2$ . Next, we calculate the derivative of Eq. (14) in respect to  $\sigma$  to find

$$\frac{\partial V_{\text{eff}}}{\partial \sigma} = \frac{2N\sigma}{\lambda} + iN \int \frac{d^4k}{(2\pi)^4} \frac{2\sigma}{\omega^2 - \xi_k^2 - |\sigma|^2}. \quad (24)$$

Using Eq. (23) in Eq. (24), we have

$$\frac{\partial V_{\text{eff}}}{\partial \sigma} = \frac{2N\sigma}{\lambda} - 2ND(k_F)\sigma \ln \left( \frac{2\Lambda}{|\sigma|} \right). \quad (25)$$

In order to calculate  $V_{\text{eff}}[\sigma]$ , we use the identity

$$V_{\text{eff}}[\sigma] = \int_0^\sigma \frac{\partial V_{\text{eff}}}{\partial \sigma'} d\sigma' + V_0, \quad (26)$$

where  $V_0$  is an arbitrary constant, which we consider to vanish, without loss of generality. Finally, using Eq. (25) in Eq. (26) and integrating over  $\sigma'$ , we obtain

$$V_{\text{eff}}[\sigma] = \frac{N\sigma^2}{\lambda} - \frac{ND(k_F)\sigma^2}{2} - ND(k_F)\sigma^2 \ln\left(\frac{2\Lambda}{|\sigma|}\right). \quad (27)$$

In Fig. 1, we plot the effective potential and discuss the energetically favorable solution. The main results are very close to the Landau-Ginzburg theory.

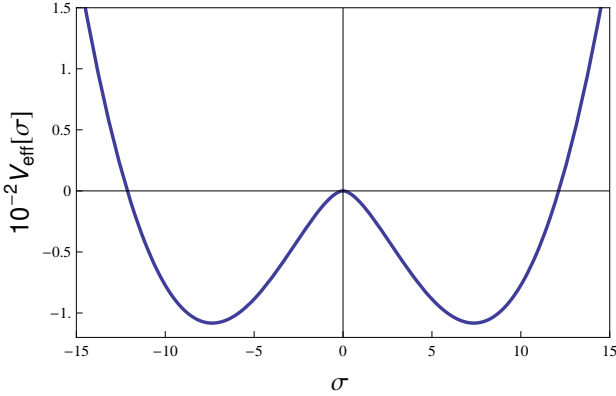


FIG. 1: (Color online) **The Effective Potential**  $V_{\text{eff}}[\sigma]$ . We plot the function in Eq. (27) with  $\Lambda = 10$  (units of energy),  $\lambda = 1.0$  (units of  $\Lambda^{-1}$ ),  $D(k_F) = 1$  and  $N = 4$ . It is shown that the two solutions  $\pm|\sigma_0|$ , given by Eq. (22), of the gap equation  $V'[\sigma_0] = 0$  are energetically favorable in comparison with the symmetric solution  $\sigma = 0$ . This resembles the well known Landau-Ginzburg potential.

### II.C- The Critical Temperature

Here, we derive the critical temperature of the BCS model. In order to do so, we return to its effective potential at zero temperature in Eq. (14). Nevertheless, here, we separate the  $\omega$  and  $k$  integrals, hence,

$$V_{\text{eff}} = \frac{N|\sigma|^2}{\lambda} - iN \int \frac{d^3k}{(2\pi)^3} \int \frac{d\omega}{2\pi} \ln(-\omega^2 + \xi_k^2 + |\sigma|^2). \quad (28)$$

We shall introduce the Matsubara frequencies in the so-called imaginary-time formalism. First, let us perform a Wick rotation given by  $\omega \rightarrow -i\omega$ . Thereafter, we use  $\omega \rightarrow \omega_n = (2n+1)\pi T$ , where  $n = 0, 1, 2, \dots$  is an integer and

$$\int \frac{d\omega}{2\pi} (\dots) \rightarrow T \sum_n (\dots). \quad (29)$$

Therefore, Eq. (28) reads

$$V_{\text{eff}}[\sigma, T] = \frac{N|\sigma|^2}{\lambda} - NT \sum_{n=-\infty}^{+\infty} \int \frac{d^3k}{(2\pi)^3} \ln(\omega_n^2 + \xi_k^2 + |\sigma|^2), \quad (30)$$

which is the effective potential of the BCS model at finite temperature.

From the first derivative of Eq. (30) in respect to  $\sigma$  calculated at  $\sigma = \sigma_0$ , we find

$$\frac{1}{\lambda} = T \sum_{n=-\infty}^{+\infty} \int \frac{d^3k}{(2\pi)^3} \frac{1}{\omega_n^2 + \xi_k^2 + |\sigma_0|^2}. \quad (31)$$

Next, we use the following identity

$$\sum_{n=-\infty}^{+\infty} \frac{1}{\omega_n^2 + \xi_k^2 + |\sigma_0|^2} = \frac{\tanh\left(\sqrt{\xi_k^2 + \sigma_0^2}/2T\right)}{2T\sqrt{\xi_k^2 + \sigma_0^2}} \quad (32)$$

in order to solve the Matsubara sum in Eq. (31). On the other hand, we may use that  $\tanh(\beta z/2) = 1 - 2n_F(z)$  for  $z \equiv \sqrt{\xi_k^2 + \sigma_0^2}$ ,  $\beta = 1/T$ , where  $n_F(z) = 1/(1 + e^{\beta z})$  is the Fermi-Dirac distribution in Eq. (32). Having these properties in mind, Eq. (31) yields

$$\frac{1}{\lambda} = \frac{1}{2} \int \frac{d^3k}{(2\pi)^3} \frac{1}{\sqrt{\xi_k^2 + |\sigma_0|^2}} - \int \frac{d^3k}{(2\pi)^3} \frac{n_F(\sqrt{\xi_k^2 + \sigma_0^2})}{\sqrt{\xi_k^2 + \sigma_0^2}}. \quad (33)$$

Clearly, the first term in the rhs of Eq. (33) is the gap equation at zero temperature given by Eq. (17). Furthermore, the second term describes the effects of the thermal bath and goes to zero as  $T \rightarrow 0$ .

Similarly to the previous case, we apply the approximation  $\int \frac{d^3k}{(2\pi)^3} \rightarrow \int_0^\Lambda d\xi_k N_s D(k_F)$ . Therefore, Eq. (31) reads

$$\frac{1}{\lambda} \approx D(k_F) \int_0^\Lambda d\xi_k \frac{\tanh\left(\sqrt{\xi_k^2 + \sigma_0^2}/2T\right)}{\sqrt{\xi_k^2 + \sigma_0^2}}, \quad (34)$$

where we have replaced  $\omega_D \rightarrow \Lambda$ . The critical temperature  $T_c$  is defined as the temperature in which the gap  $\sigma_0$  vanishes. This is determined by Eq. (34), hence,

$$\frac{1}{\lambda} \approx D(k_F) \int_0^\Lambda d\xi_k \frac{\tanh(\xi_k/2T_c)}{\xi_k}. \quad (35)$$

Next, let us define  $y \equiv \xi_k/(2T_c)$ . Therefore, Eq. (35) reads

$$\frac{1}{\lambda} \approx D(k_F) \int_0^{\Lambda/(2T_c)} dy \frac{\tanh(y)}{y}. \quad (36)$$

The integral over  $y$  may be calculated by parts, i.e.,

$$\int_0^{\Lambda/(2T_c)} dy \frac{\tanh(y)}{y} = \tanh(y) \ln(y) \Big|_0^{\Lambda/(2T_c)} - \int_0^{\Lambda/(2T_c)} dy \frac{\ln(y)}{\cosh^2(y)}. \quad (37)$$

Within the regime  $\Lambda \gg 2T_c$ , Eq. (37) yields

$$\begin{aligned} \int_0^{\Lambda/(2T_c)} dy \frac{\tanh(y)}{y} &\approx \ln\left(\frac{\Lambda}{2T_c}\right) - \ln\left(\frac{\pi}{4e^{\gamma_E}}\right) \\ &= \ln\left(\frac{2\Lambda e^{\gamma_E}}{\pi T_c}\right), \end{aligned} \quad (38)$$

where  $\gamma_E \approx 0.57$  is the Euler constant. Using Eq. (38) in Eq. (35), we find

$$T_c \approx \frac{2\Lambda e^{\gamma_E}}{\pi} e^{-1/\lambda D(k_F)} = |\sigma_0| \frac{e^{\gamma_E}}{\pi}, \quad (39)$$

where in the last term in the rhs of Eq. (39) we have used the expression for the gap in Eq. (22). This shows that an universal ratio for BCS superconductors is found, namely,  $|\sigma_0|/(k_B T_c) = \pi/e^{\gamma_E} \approx 1.76$ , where we have properly included the Stefan-Boltzmann constant  $k_B$ . Finally, it is well known that the typical values of  $T_c$  are on the interval 30-40K, which can not describe the high- $T_c$  superconductors where  $T_c$  may be close to 100K [4, 5].

### III. TWO-GAP APPROACH FOR THE BCS MODEL

In this section we propose a generalization of the BCS model, considering the introduction of a flavor symmetry breaking. Thereafter, we study the formation of Cooper pairs due to both inter and intra-flavor interactions. This model describes a two-gap superconductor made of two nonrelativistic electrons, similarly to what has been done in Ref. [15] for underdoped cuprate superconductors.

Our first step is to assume that the matter field is described by three indexes, i.e.,  $\psi = \psi_{sai}$ , where  $s = \uparrow, \downarrow$  describes de spin,  $a = 1, \dots, N$  is the flavor index, and  $i = K, K'$  describes an internal symmetry of the cristal, such as a sublattice symmetry. Therefore, the total symmetry is described by matrices in the group  $SU(2) \times SU(N) \times SU(2)$ . Hence, the two-gap-BCS Lagrangian reads

$$\begin{aligned} \mathcal{L}_{2G} &= \psi_{sai}^* \left( i \frac{\partial}{\partial t} - \frac{\nabla^2}{2m} \right) \psi_{sai} \\ &- \frac{\lambda}{N} \psi_{a,K,\uparrow}^* \psi_{a,K,\downarrow}^* \psi_{a,K,\downarrow} \psi_{a,K,\uparrow} \\ &- \frac{\lambda}{N} \psi_{a,K',\uparrow}^* \psi_{a,K',\downarrow}^* \psi_{a,K',\downarrow} \psi_{a,K',\uparrow} \\ &- \frac{g}{N} \psi_{a,K,\uparrow}^* \psi_{a,K',\downarrow}^* \psi_{a,K',\downarrow} \psi_{a,K,\uparrow} \\ &- \frac{g}{N} \psi_{a,K',\uparrow}^* \psi_{a,K,\downarrow}^* \psi_{a,K,\downarrow} \psi_{a,K',\uparrow}, \end{aligned} \quad (40)$$

where we shall call  $\lambda$  as intra-flavor coupling constant and  $g$  as inter-flavor coupling constant in reference to the new indexes  $K, K'$ .

$$\begin{aligned} \mathcal{L}_{2G} &\rightarrow \mathcal{L}_{2G} + \frac{N}{\lambda} \left( \sigma_K + \frac{\lambda}{N} \psi_{a,K,\uparrow}^* \psi_{a,K,\downarrow}^* \right) \\ &\times \left( \sigma_K^* + \frac{\lambda}{N} \psi_{a,K,\downarrow} \psi_{a,K,\uparrow} \right) \\ &+ \frac{N}{\lambda} \left( \sigma_{K'} + \frac{\lambda}{N} \psi_{a,K',\uparrow}^* \psi_{a,K',\downarrow}^* \right) \\ &\times \left( \sigma_{K'}^* + \frac{\lambda}{N} \psi_{a,K',\downarrow} \psi_{a,K',\uparrow} \right) \\ &+ \frac{N}{g} \left( \Delta_{KK'} + \frac{g}{N} \psi_{a,K,\uparrow}^* \psi_{a,K',\downarrow}^* \right) \\ &\times \left( \Delta_{KK'}^* + \frac{g}{N} \psi_{a,K',\downarrow} \psi_{a,K,\uparrow} \right) \\ &+ \frac{N}{g} \left( \Delta_{K'K} + \frac{g}{N} \psi_{a,K',\uparrow}^* \psi_{a,K,\downarrow}^* \right) \\ &\times \left( \Delta_{K'K}^* + \frac{g}{N} \psi_{a,K,\downarrow} \psi_{a,K',\uparrow} \right). \end{aligned} \quad (41)$$

From the motion equation for the auxiliary fields  $\sigma_K, \sigma_{K'}$ ,  $\Delta_{KK'}$ , and  $\Delta_{K'K}$ , we find

$$\sigma_K^0 = -\frac{\lambda}{N} \langle \psi_{a,K,\downarrow}^* \psi_{a,K,\uparrow}^* \rangle, \quad (42)$$

$$\sigma_{K'}^0 = -\frac{\lambda}{N} \langle \psi_{a,K',\downarrow}^* \psi_{a,K',\uparrow}^* \rangle, \quad (43)$$

$$\Delta_{KK'}^0 = -\frac{g}{N} \langle \psi_{a,K',\downarrow}^* \psi_{a,K,\uparrow}^* \rangle, \quad (44)$$

and

$$\Delta_{K'K}^0 = -\frac{g}{N} \langle \psi_{a,K,\downarrow}^* \psi_{a,K',\uparrow}^* \rangle, \quad (45)$$

which are our four order parameters for the two-gap BCS model, where the index 0 refers to the vacuum expectation value for each of them. Note that the expectation values of  $\sigma_K^0$  describes the intra-flavor symmetry breaking while  $\Delta_{KK'}^0$  defines the inter-flavor symmetry breaking phase.

Following the same steps as before, after we use the Hubbard-Stratonovich transformation in Eq. (41), we find

$$\begin{aligned} \mathcal{L}_{2G} &= \psi_{sai}^* \left( i \frac{\partial}{\partial t} - \frac{\nabla^2}{2m} \right) \psi_{sai} \\ &+ \frac{N|\sigma_K|^2}{\lambda} + \frac{N|\sigma_{K'}|^2}{\lambda} + \frac{N|\Delta_{KK'}|^2}{g} + \frac{N|\Delta_{K'K}|^2}{g} \\ &+ \sigma_K \psi_{a,K,\downarrow} \psi_{a,K,\uparrow} + \sigma_K^* \psi_{a,K,\uparrow}^* \psi_{a,K,\downarrow}^* \\ &+ \sigma_{K'} \psi_{a,K',\downarrow} \psi_{a,K',\uparrow} + \sigma_{K'}^* \psi_{a,K',\uparrow}^* \psi_{a,K',\downarrow}^* \\ &+ \Delta_{KK'} \psi_{a,K',\downarrow} \psi_{a,K,\uparrow} + \Delta_{KK'}^* \psi_{a,K,\uparrow}^* \psi_{a,K',\downarrow}^* \\ &+ \Delta_{K'K} \psi_{a,K,\downarrow} \psi_{a,K',\uparrow} + \Delta_{K'K}^* \psi_{a,K',\uparrow}^* \psi_{a,K,\downarrow}^*. \end{aligned} \quad (46)$$

Note that Eq. (46) is quadratic in the Nambu field, namely,  $\Phi_a^\dagger = (\psi_{a,K,\uparrow}^* \psi_{a,K,\downarrow} \psi_{a,K',\uparrow}^* \psi_{a,K',\downarrow})$ .

### III.A-The Effective Potential

The main step is to observe that Eq. (46) may be written as

$$\mathcal{L}_{2G} = \Phi_a^\dagger \hat{K}_{2G} \Phi_a + \frac{N|\sigma_K|^2}{\lambda} + \frac{N|\sigma_{K'}|^2}{\lambda} + \frac{N|\Delta_{KK'}|^2}{g} + \frac{N|\Delta_{K'K}|^2}{g}, \quad (47)$$

where

$$\hat{K}_{2G} = \begin{pmatrix} \xi_\nabla + \omega_t & \sigma_K^* & 0 & \Delta_{K'K} \\ \sigma_K & -\xi_\nabla + \omega_t & \Delta_{KK'} & 0 \\ 0 & \Delta_{KK'}^* & \xi_\nabla + \omega_t & \sigma_{K'}^* \\ \Delta_{K'K} & 0 & \sigma_{K'} & -\xi_\nabla + \omega_t \end{pmatrix} \quad (48)$$

with  $\omega_t \equiv i\partial/\partial t$  and  $\xi_\nabla \equiv \nabla^2/2m$ .

Following the same steps as in the previous section, after we integrate over the field  $\Phi_a$  in Eq. (47), we obtain the effective potential

$$V_{\text{eff}}^{2G} = -iN \ln \det[-i\hat{K}_{2G}] + \frac{N|\sigma_K|^2}{\lambda} + \frac{N|\sigma_{K'}|^2}{\lambda} + \frac{N|\Delta_{KK'}|^2}{g} + \frac{N|\Delta_{K'K}|^2}{g}. \quad (49)$$

Next, we consider that  $\sigma_K = \sigma_{K'} = \sigma$  and  $\Delta_{KK'} = \Delta_{K'K} = \Delta$ , which is reasonable because we only take two independent coupling constants  $\lambda$  and  $g$ . In this case, from Eq. (48), it is straightforward that  $\det[-i\hat{K}_{2G}] = \ln(-\omega^2 + \xi_k^2 + |X|^2) + \ln(-\omega^2 + \xi_k^2 + |Y|^2)$ , where  $X = \sigma + \Delta$  and  $Y = \sigma - \Delta$ . Using this result in Eq. (49), we find

$$V_{\text{eff}}^{2G}[\sigma, \Delta] = \frac{2N|\sigma|^2}{\lambda} + \frac{2N|\Delta|^2}{g} - iN \int \frac{d^4k}{(2\pi)^4} \ln(-\omega^2 + \xi_k^2 + |X|^2) - iN \int \frac{d^4k}{(2\pi)^4} \ln(-\omega^2 + \xi_k^2 + |Y|^2). \quad (50)$$

When we take  $\Delta \rightarrow 0$  in Eq. (52), we find the effective potential of the BCS model, given in Eq. (14), multiplied by an overall factor of 2, which is due to the new index  $i = K, K'$ . The gap equation, however, is the same, as expected. Next, let us discuss the case when  $\Delta \neq 0$ .

From the approximations we applied in the BCS model, by comparison of Eq. (14) with Eq. (27), we conclude that

$$-iN \int \frac{d^4k}{(2\pi)^4} \ln(-\omega^2 + \xi_k^2 + |Z|^2) \approx -\frac{ND(k_F)Z^2}{2} - ND(k_F)Z^2 \ln\left(\frac{2\Lambda}{|Z|}\right) + V_0, \quad (51)$$

where  $Z$  is an arbitrary real constant and  $V_0$  a constant that does not depend on  $Z$  (which we shall neglect for

the sake of simplicity). Using Eq. (51) in Eq. (52), we find

$$V_{\text{eff}}^{2G}[\sigma, \Delta] = \frac{2N\sigma^2}{\lambda} + \frac{2N\Delta^2}{g} - \frac{ND(k_F)X^2}{2} - ND(k_F)X^2 \ln\left(\frac{2\Lambda}{|X|}\right) - \frac{ND(k_F)Y^2}{2} - ND(k_F)Y^2 \ln\left(\frac{2\Lambda}{|Y|}\right) \quad (52)$$

which holds when  $(\sigma, \Delta)$  are real constants.

### III.B-The Coupled-Gap Equations

The gap equation is now obtained by extremizing the effective potential in respect to both fields  $\sigma$  and  $\Delta$ , i.e., we have to calculate

$$\frac{\partial V_{\text{eff}}^{2G}}{\partial \sigma} \Big|_{\sigma=\sigma_0, \Delta_0} = 0 \quad (53)$$

and

$$\frac{\partial V_{\text{eff}}^{2G}}{\partial \Delta} \Big|_{\Delta=\Delta_0, \sigma_0} = 0. \quad (54)$$

Clearly, Eq. (53) and Eq. (54) are two independent equations that provide the solutions for  $\sigma_0$  and  $\Delta_0$ . These are the minimum of the effective potential. After summing Eq. (53) and Eq. (54), we find

$$4N \left[ \frac{\Delta_0}{g} + \frac{\sigma_0}{\lambda} - D(k_F)X_0 \ln\left(\frac{2\Lambda}{|X_0|}\right) \right] = 0, \quad (55)$$

where  $X_0 = \sigma_0 + \Delta_0$ . On the other hand, by calculating the subtraction between Eq. (53) and Eq. (54), we obtain

$$4N \left[ -\frac{\Delta_0}{g} + \frac{\sigma_0}{\lambda} - D(k_F)Y_0 \ln\left(\frac{2\Lambda}{|Y_0|}\right) \right] = 0, \quad (56)$$

where  $Y_0 = \sigma_0 - \Delta_0$ . From Eq. (55) and Eq. (56), we conclude that  $|X_0| = |Y_0|$  when  $g = \lambda$ , hence,  $\Delta_0 = 0$  and we obtain the standard BCS model of the previous section. Because of that, from now on, let us assume  $g \neq \lambda$  and discuss the competition between  $\sigma_0$  and  $\Delta_0$ .

Interesting, both Eq. (55) and Eq. (56) define a critical gap  $\Delta_0^c$ , where  $\sigma_0 = 0$  for  $\Delta \geq \Delta_0^c$  and  $\sigma_0 \neq 0$  for  $\Delta < \Delta_0^c$ . In order to calculate  $\Delta_0^c$ , we consider  $\sigma_0 = 0$  in Eq. (55) and, after a simple algebra, we have

$$\Delta_0^c = 2\Lambda e^{-1/D(k_F)g}. \quad (57)$$

Note that Eq. (57) may also be obtained, following the same steps, from Eq. (56).

In Fig. 2 we show how the minimum  $\sigma_0$  changes as we cross the point  $\Delta_0^c$ . Indeed, for  $\Delta < \Delta_0^c$  the effective potential resembles Fig. 1 and we find two well distinct points  $\pm|\sigma_0|$ , which is shown in the dashed line. On the

other hand, for  $\Delta \geq \Delta_0^c$ , the minimum of the effective potential is shown to be given by  $\sigma_0 = 0$ , providing a normal phase that is shown by the common line. Furthermore, we also consider a case where  $\Delta \approx \Delta_0^c$  (the inset of Fig. 2), which shows that at this point the solutions  $-|\sigma_0|$  and  $+|\sigma_0|$  are almost connected by a line, which means that the system is going to the normal phase.

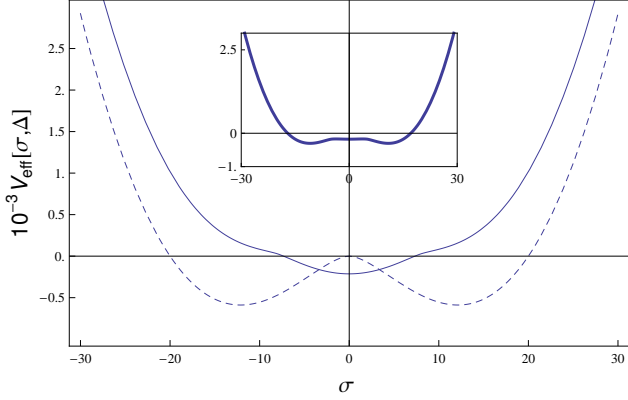


FIG. 2: (Color online) **The Effective Potential**  $V_{\text{eff}}^{2G}[\sigma, \Delta]$ . We plot the function in Eq. (52) with  $\Lambda = 10$  (units of energy),  $\lambda = 1.0$  (units of  $\Lambda^{-1}$ ),  $D(k_F) = 1$ ,  $g = 2$  (units of  $\Lambda^{-1}$ ), and  $N = 4$ . Using these parameters, Eq. (57) provides  $\Delta_0^c \approx 7.4$  (units of  $\Lambda$ ). In the dashed line we use  $\Delta = 0.1$  ( $\Delta < \Delta_0^c$ ) while for the common line we use  $\Delta = 8.0$  ( $\Delta \geq \Delta_0^c$ ). The inset shows an extra figure with  $\Delta = 5.0$  ( $\Delta \approx \Delta_0^c$ ), representing an intermediate case.

### III.C-The Critical Temperature

We would like to calculate the critical temperature  $T_{c2}$  in which the  $\sigma_0$ -gap vanishes. After introducing the Matsubara frequencies, as we did before in Sec. II, we find

$$\begin{aligned} V_{\text{eff}}^{2G}[\sigma, \Delta, T] &= \frac{2N|\sigma|^2}{\lambda} + \frac{2N|\Delta|^2}{g} \\ &- NT \sum_{n=-\infty}^{\infty} \int \frac{d^3k}{(2\pi)^3} \ln(\omega_n^2 + \xi_k^2 + |X|^2) \\ &- NT \sum_{n=-\infty}^{\infty} \int \frac{d^3k}{(2\pi)^3} \ln(\omega_n^2 + \xi_k^2 + |Y|^2), \end{aligned} \quad (58)$$

which is the effective potential of the two-gap BCS model at finite temperature. Similarly to the zero temperature case, we have two-coupled gap equations, namely,

$$\frac{\partial V_{\text{eff}}^{2G}[T]}{\partial \sigma} \Big|_{\sigma=\sigma_0, \Delta_0} = 0 \quad (59)$$

and

$$\frac{\partial V_{\text{eff}}^{2G}[T]}{\partial \Delta} \Big|_{\Delta=\Delta_0, \sigma_0} = 0. \quad (60)$$

For the sake of simplicity we assume that both  $\sigma$  and  $\Delta$  are real constants. Therefore, these gap equations are given by

$$\begin{aligned} \frac{4N\sigma_0}{\lambda} - NT \sum_{n=-\infty}^{\infty} \int \frac{d^3k}{(2\pi)^3} \frac{2X_0}{\omega_n^2 + \xi_k^2 + |X_0|^2} \\ - NT \sum_{n=-\infty}^{\infty} \int \frac{d^3k}{(2\pi)^3} \frac{2|Y_0|}{\omega_n^2 + \xi_k^2 + |Y_0|^2} = 0 \end{aligned} \quad (61)$$

and

$$\begin{aligned} \frac{4N\Delta_0}{g} - NT \sum_{n=-\infty}^{\infty} \int \frac{d^3k}{(2\pi)^3} \frac{2X_0}{\omega_n^2 + \xi_k^2 + |X_0|^2} \\ + NT \sum_{n=-\infty}^{\infty} \int \frac{d^3k}{(2\pi)^3} \frac{2|Y_0|}{\omega_n^2 + \xi_k^2 + |Y_0|^2} = 0, \end{aligned} \quad (62)$$

respectively.

From Eq. (61) and Eq. (62), we conclude that

$$\begin{aligned} \frac{4N\sigma_0}{\lambda} + \frac{4N\Delta_0}{g} \\ - 2NT \sum_{n=-\infty}^{\infty} \int \frac{d^3k}{(2\pi)^3} \frac{2X_0}{\omega_n^2 + \xi_k^2 + |X_0|^2} = 0. \end{aligned} \quad (63)$$

The sum over  $\omega_n$  may be solved with the help of Eq. (32). Furthermore, we also replace  $\int \frac{d^3k}{(2\pi)^3} \rightarrow \int_0^\Lambda d\xi_k N_s D(k_F)$  to obtain

$$\begin{aligned} \frac{\sigma_0}{\lambda} + \frac{\Delta_0}{g} \\ \approx X_0 D(k_F) \int_0^\Lambda d\xi_k \frac{\tanh\left[\frac{\sqrt{\xi_k^2 + X_0^2}}{2T}\right]}{\sqrt{\xi_k^2 + X_0^2}}. \end{aligned} \quad (64)$$

Next, we use  $T = T_{c2}$  and  $\sigma_0 = 0$  in Eq. (64). Note that this implies  $X_0 = \Delta_0$ . Therefore, we find

$$\frac{1}{gD(k_F)} \approx \int_0^\Lambda d\xi_k \frac{\tanh\left[\frac{\sqrt{\xi_k^2 + \Delta_0^2}}{2T_{c2}}\right]}{\sqrt{\xi_k^2 + \Delta_0^2}}. \quad (65)$$

We may define  $z \equiv \sqrt{\xi_k^2 + \Delta_0^2}/(2T_{c2})$ , such that Eq. (65) reads

$$\frac{1}{gD(k_F)} \approx \int_{|\Delta_0|/2T_{c2}}^{\sqrt{\Lambda^2 + \Delta_0^2}/2T_{c2}} dz \frac{\tanh[z]}{\sqrt{z^2 - [\Delta_0/(2T_{c2})]^2}}. \quad (66)$$

Note that Eq. (66) resembles Eq. (36) when  $\Delta_0 = 0$ . Because of this, we may follow the same steps as in Eqs. (36)-(39) when we consider  $\Lambda \gg T_{c2}, \Delta_0$ . Hence, after some algebra, we obtain

$$T_{c2} \approx \frac{2\Lambda e^{\gamma_E}}{\pi} e^{-1/gD(k_F)} = \Delta_0^c \frac{e^{\gamma_E}}{\pi}, \quad (67)$$

where we have used Eq. (57) in the last term of Eq. (67). The physical interpretation of  $T_{c2}$  is quite simple. Indeed,

as we have shown in the previous section, the larger is the value of  $\Delta_0^c$  more easily the system goes to a broken phase (see Fig. (2)) and, therefore, the larger will be its critical temperature. Obviously, despite the simplicity of the two-gap BCS model, we are assuming that we actually may control the value of  $g$  (and  $\Delta_g^c$ ), which in real experiments may be a hard task [18]

#### IV. CONCLUSIONS

In this work we have described the solutions of a two-gap problem in a continuum version of the BCS model, using a finite ultraviolet cutoff  $\Lambda$ . Our main result shows that the extra gap  $\Delta$  restores the symmetric phase when  $\Delta \geq \Delta_0^c$ , where  $\Delta_0^c$  is a critical parameter, and for  $\Delta < \Delta_0^c$  the system is in the superconductor phase. The value of  $\Delta_0^c$  also defines the critical temperature  $T_{c2}$  for the superconductor phase in the system with two gaps. This conclusion is corroborated by an analysis of the effective potential at the large- $N$  approximation. The two-gap BCS model [15] is expected to be relevant for describing unconventional pairing in superconductors with high- $T_c$ , for example, in MgB2 and underdoped cuprates [19]. This, unfortunately, has been less discussed in literature. Here, we gave a step forward by considering its continuum version.

The large- $N$  approximation that we applied in this work resembles more quantum-field-theory methods than condensed matter physics. This happens because we have neglected several microscopic informations about hybridization, for example, of the electronic bands. In principle, one concludes that this level of approximation is too far from reality. Fortunately, this seems not to be the case. Indeed, it has been shown that a quantum-field-theory description of the Fermi velocity renormalization in graphene [20] yields a good agreement with experimental data [21]. Furthermore, the application of Pseudo quantum electrodynamics [22] for describing excitonic spectrum (pairs of electron and hole) in transition metal dichalcogenides has also been shown very useful [8]. Therefore, it is clear that there exist a window of applicability for such approximations in electronic properties of a crystal. In general, for a better comparison with experiments, we may assume that we must neglect impurities, disorder, lattice vibrations, and higher-order-momentum dependence in the energy dispersion. Although it is possible to improve the approximations for taking into account all of these effects, a full model describing these features is yet to be found.

#### Acknowledgments

L. O. N. is partially supported by Conselho Nacional de Desenvolvimento Científico e Tecnológico (CNPq) and

by CAPES/NUFFIC, finance code 0112. L. O. N. thanks V. S. Alves, C. M. Smith, and E. C. Marino for several insightful discussions.

#### APPENDIX A: THE EFFECTIVE ACTION WITHIN THE LARGE- $N$ EXPANSION

In this appendix, we give an introduction to the large- $N$  expansion in the light of the effective action for the auxiliary field. This is useful for a better understanding of the approximation as well as for clarifying the meaning of the effective potential we have calculate so far. Our steps are the same as in Ref. [2]. First, we perform a shift on the field  $\sigma(x) \rightarrow \sigma_0 + \sigma(x)/\sqrt{N}$  with  $\langle \sigma \rangle = \sigma_0$  in Eq. (6). Therefore, we obtain

$$\begin{aligned} \mathcal{L}_{\text{BCS}} = & \Phi_a^\dagger \left( i \frac{\partial}{\partial t} - \frac{\nabla^2}{2m} \sigma_0 + \frac{\sigma}{\sqrt{N}} \right) \Phi_a \\ & + \frac{\sqrt{N} \sigma_0 \sigma^*}{\lambda} + \frac{\sqrt{N} \sigma \sigma_0^*}{\lambda} + \frac{\sigma \sigma^*}{\lambda}, \end{aligned} \quad (68)$$

where the Nambu fermion field is given by  $\Phi_a^\dagger = (\psi_{a,\uparrow}^\dagger, \psi_{a,\downarrow})$ . Using Eq. (10) we may solve the integral over  $\Phi_a$  in Eq. (68) and obtain the effective action for the field  $\sigma$ , namely,

$$\begin{aligned} \mathcal{L}_{\text{eff}}[\sigma] = & -iN \ln \left[ (|\sigma_0|^2 - S_\psi^2) + \frac{\sigma \sigma_0^*}{\sqrt{N}} + \frac{\sigma^* \sigma_0}{\sqrt{N}} - \frac{|\sigma|^2}{N} \right] \\ & + \frac{\sqrt{N} \sigma_0 \sigma^*}{\lambda} + \frac{\sqrt{N} \sigma \sigma_0^*}{\lambda} + \frac{\sigma \sigma^*}{\lambda}, \end{aligned} \quad (69)$$

where the function  $S_\psi^2$  reads

$$S_\psi^2 = -\frac{\partial^2}{\partial t^2} - \left[ \frac{\nabla^2}{2m} \right]^2. \quad (70)$$

We may expand the logarithmic term in Eq. (69) by assuming that  $N$  is large ( $N \gg 1$ ) [2], such that we obtain

$$\mathcal{L}_{\text{eff}}[\sigma] = \sqrt{N} \mathcal{L}_0[\sigma] + N^0 \mathcal{L}_1[\sigma] + O(1/\sqrt{N}), \quad (71)$$

where we shall neglect the terms  $O(1/\sqrt{N})$ . This series expansion is easily performed by using  $\ln(1+x) \approx x - x^2/2 + \dots$  for  $|x| \ll 1$ , where

$$x \equiv \frac{\left( \frac{\sigma \sigma_0^*}{\sqrt{N}} + \frac{\sigma^* \sigma_0}{\sqrt{N}} - \frac{|\sigma|^2}{N} \right)}{(|\sigma_0|^2 - S_\psi^2)}. \quad (72)$$

Therefore, after some algebra, we find

$$\begin{aligned} \mathcal{L}_0[\sigma] = & \frac{\sigma_0 \sigma^*}{\lambda} + \frac{\sigma \sigma_0^*}{\lambda} \\ & + i \left[ (S_\psi^2 - |\sigma_0|^2)^{-1} (\sigma_0 \sigma^* + \sigma \sigma_0^*) \right], \end{aligned} \quad (73)$$



and

$$\begin{aligned} \mathcal{L}_1[\sigma] &= \frac{\sigma\sigma^*}{\lambda} + i[(S_\psi^2 - |\sigma_0|^2)^{-1}\sigma\sigma^*] \\ &+ \frac{i}{2}[(S_\psi^2 - |\sigma_0|^2)^{-2}(\sigma_0\sigma^* + \sigma\sigma_0^*)^2]. \end{aligned} \quad (74)$$

Within this large- $N$  limit, we must assume that  $\mathcal{L}_0[\sigma] = 0$ , which is our gap equation, otherwise the series expansion in Eq. (71) does not converge.

From  $\mathcal{L}_0[\sigma] = 0$  and Eq. (73), we conclude that

$$-\frac{1}{\lambda} = i \frac{1}{(S_\psi^2 - |\sigma_0|^2)}. \quad (75)$$

The Fourier transform of Eq. (75) is exactly Eq. (16), as expected. In particular, we note that the effective potential, as in general, may be written as

$$V_{\text{eff}}[\sigma] = \int_0^\sigma \mathcal{L}_0[\sigma'] d\sigma' + V_0, \quad (76)$$

which means that  $V_{\text{eff}}[\sigma]$  is, essentially, given by the integral of the gap equation. This explains why we were able to calculate an explicit expression for this quantity in Eq. (27) with the help of Eq. (26). In principle, one could follow our expansion in Eq. (71) and calculate higher-order corrections at any order of  $N$ , which may not be a trivial task [2].

---

\* Electronic address: [lon@ufpa.br](mailto:lon@ufpa.br)

- [1] M. D. Schwartz, *Quantum Field Theory and the Standard Model*, Cambridge University Press (2014).
- [2] Sidney Coleman, *Aspects of Symmetry*, Cambridge University Press, (1985).
- [3] R. T. Cahill and C. D. Roberts, *Soliton bag models of hadrons from QCD*, Phys. Rev. D **32**, 2419 (1985).
- [4] A. M. J. Schakel, *Boulevard of Broken Symmetries Effective Field Theories of Condensed Matter*, World Scientific, (2008).
- [5] Eduardo C. Marino, *Quantum Field Theory Approach to Condensed Matter Physics*, Cambridge University Press, (2017).
- [6] J. Bardeen, L. N. Cooper, and J. R. Schrieffer, *Theory of Superconductivity*, Phys. Rev. **108**, 1175 (1957).
- [7] L. Rademaker, *A Practical Introduction to Density Functional Theory*, arxiv: 2011.09888 (2020).
- [8] E. C. Marino, L.O. Nascimento, Van Sergio Alves, N. Menezes, and C.M. Smith, *Quantum-electrodynamical approach to the exciton spectrum in transition-metal dichalcogenides*, 2D Materials **5**, 041006 (2018).
- [9] E. C. Marino, L. O. Nascimento, V. S. Alves, and C. M. Smith, *Interaction Induced Quantum Valley Hall Effect in Graphene*, Phys. Rev. X **5**, 011040 (2015).
- [10] K. S. Novoselov, A. K. Geim, S. V. Morozov, D. Jiang, Y. Zhang, S. V. Dubong, I. V. Grigorieva, and A. A. Firsov, *Electric Field Effect in Atomically Thin Carbon Films*, Science **306**, 666, (2004).
- [11] B. Lalmi, H. Oughaddou, H. Enriquez, A. Kara, S. Vizzini, B. Ealet, and B. Aufray, *Epitaxial growth of a silicene sheet*, Appl. Phys. Lett. **97**, 223109 (2010).
- [12] Gang Wang, Alexey Chernikov, Mikhail M. Glazov, Tony F. Heinz, Xavier Marie, Thierry Amand, and Bernhard Urbaszek, *Excitons in atomically thin transition metal dichalcogenides*, in press Review of Modern Physics (2018).
- [13] B. A. Bernevig with T. Hughes, *Topological Insulators and Topological Superconductors*. Princeton University Press, (2013); S.-Q. Shen, *Topological Insulators Dirac Equation in Condensed Matter*, Spring Series in Solid-State Sciences, (2012); M. Z. Hasan and C. L. Kane, *Colloquium: Topological Insulators*, Rev. Mod. Phys. **82**, 3045, (2010).
- [14] E. C. Marino, R. O. Correa Jr, R. Arouca, L. H. C. M. Nunes, and V. S. Alves, *Superconducting and Pseudogap Transition Temperatures in High- $T_c$  Cuprates and the  $T_c$  Dependence on Pressure*, arXiv:1908.07028v2 (2020). Accepted for publication.
- [15] A. Perali, C. Castellani, C. Di Castro, M. Grilli, E. Piegari, and A. A. Varlamov, *Two-gap model for underdoped cuprate superconductors*, Phys. Rev. D **62**, R9295 (2010).
- [16] J. Chen, L. Jiao, J. L. Zhang, Y. Chen, L. Yang, M. Nicklas, F. Steglich, and H. Q. Yuan, *Evidence for two-gap superconductivity in the non-centrosymmetric compound  $\text{LaNiC}_2$* , New Journal of Physics **15**, 053005 (2013).
- [17] T. Wang, Y. Ma, W. Li, J. Chu, L. Wang, J. Feng, H. Xiao, Z. Li, T. Hu, X. Liu, and G. Mu, *Two-gap superconductivity in  $\text{CaFe}_{0.88}\text{Co}_{0.12}\text{AsF}$  revealed by temperature dependence of the lower critical field  $H_{c1c}(T)$* , Quantum Materials **4**, article number 33 (2019).
- [18] O. Hart, G. Goldstein, C. Chamon, and C. Castellano, *Steady-state superconductivity in electronic materials with repulsive interactions*, Phys. Rev. B **100**, 060508(R) (2019).
- [19] J. Nagamatsu, N. Nakagawa, T. Muranaka, Y. Zenitani, and J. Akimitsu, Nature **410**, *Superconductivity at 39 K in magnesium diboride*, 63 (2001);
- [20] M. A. H. Vozmediano and F. Guinea, *Effect of Coulomb Interactions on the Physical Observables of Graphene*, Phys. Scr. **T146**, 014015 (2012); F. de Juan, A. G. Grushin, and M. A. H. Vozmediano, *Renormalization of Coulomb Interaction in Graphene: Determining Observable Quantities*, Phys. Rev. B **82**, 125409 (2010).
- [21] D. C. Elias, R. V. Gorbachev, A. S. Mayorov, S. V. Morozov, A. A. Zhukov, P. Blake, L. A. Ponomarenko, I. V. Grigorieva, K. S. Novoselov, F. Guinea, and A. K. Geim, *Dirac Cones Reshaped by Interaction Effects in Suspended Graphene*, Nat. Phys. **7**, 701-704 (2011).
- [22] L. O. Nascimento, *Introduction to Topological Phases and Electronic Interactions in (2+1) Dimensions*, Brazilian Journal of Physics **47**, 215-230 (2017).